# Quantum Error Correction, and Z(2) Gauge Theories

Seyong Kim
Sejong University

In collaboration with M. Mueller (IQI, RWTH), M. Rispler (IQI, RWTH) and D. Vodola (BASF)

Quantum 6 (2022) 618, and a work in progress

# Optica 11 (2024) 2222

222 Vol. 11, No. 2 / February 2024 / *Optica* **Research Article**

Check for updates

OPTICA

## Supercharged two-dimensional tweezer array with more than 1000 atomic qubits

**Lars Pause,[1] Lukas Sturm,[1] Marcel Mittenbühler,[1] Stephan Amann,[1,2] Tilman Preuschoff,[1] Dominik Schäffner,[1] Malte Schlosser,[1] and Gerhard Birkl[1,*]**

[1] *Technische Universität Darmstadt, Institut für Angewandte Physik, Schlossgartenstraße 7, 64289 Darmstadt, Germany*
[2] *Current address: Max-Planck-Institut für Quantenoptik, Hans-Kopfermann-Straße 1, 85748 Garching, Germany*
**apqpub@physik.tu-darmstadt.de*

*Received 16 November 2023; revised 12 January 2024; accepted 19 January 2024; published 7 February 2024*

We report on the realization of a large-scale quantum-processing architecture surpassing the tier of 1000 atomic qubits. By tiling multiple microlens-generated tweezer arrays, each operated by an independent laser source, we can eliminate laser-power limitations in the number of allocatable qubits. Already with two separate arrays, we implement combined 2D configurations of 3000 qubit sites with a mean number of 1167(46) single-atom quantum systems. The transfer of atoms between the two arrays is achieved with high efficiency. Thus, supercharging one array designated as the quantum

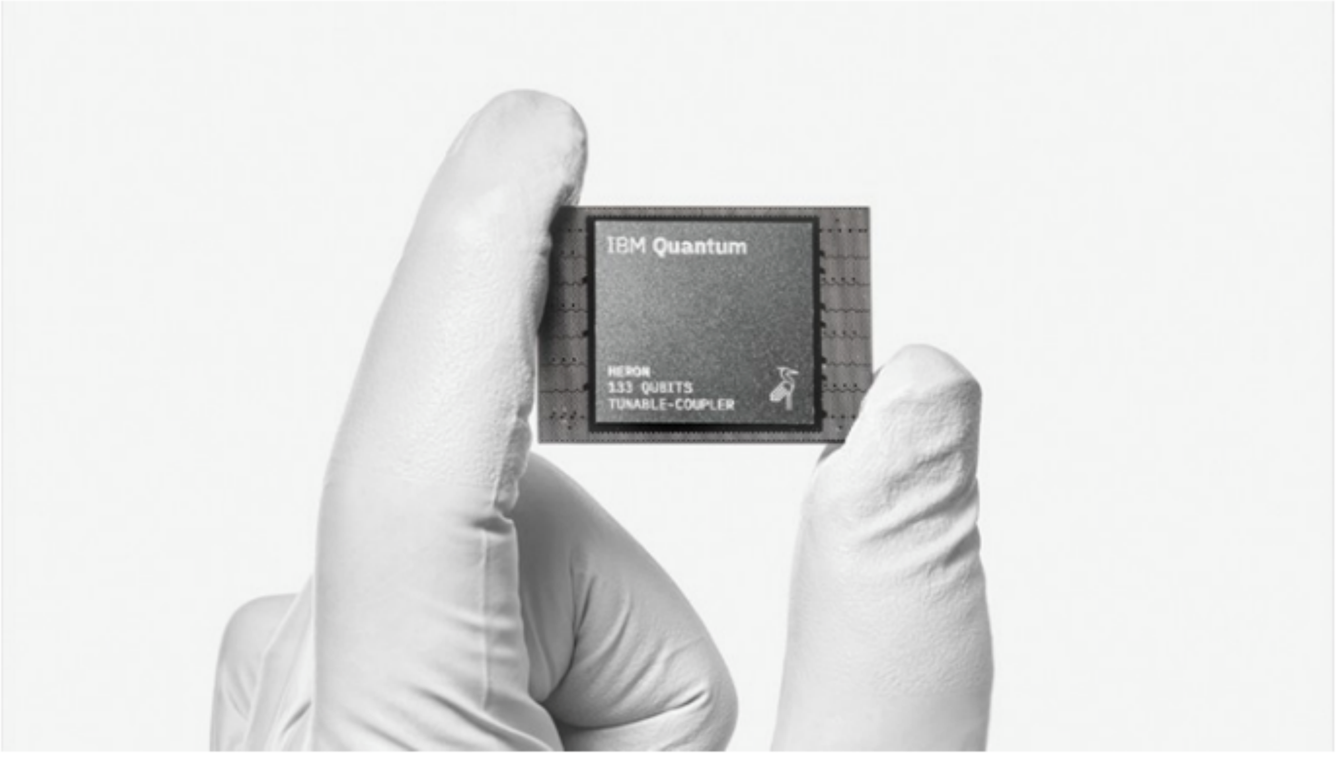


In its latest quantum processor, called Heron, IBM has improved the reliability of the qubits. Credit: Ryan Lavine for IBM

IBM has unveiled the first quantum computer with more than 1,000 qubits – the equivalent of the digital bits in an ordinary computer. But the company says that it will now shift gears and focus on making its machines more error-resistant rather than larger.

# Nature 624 (2023) 238

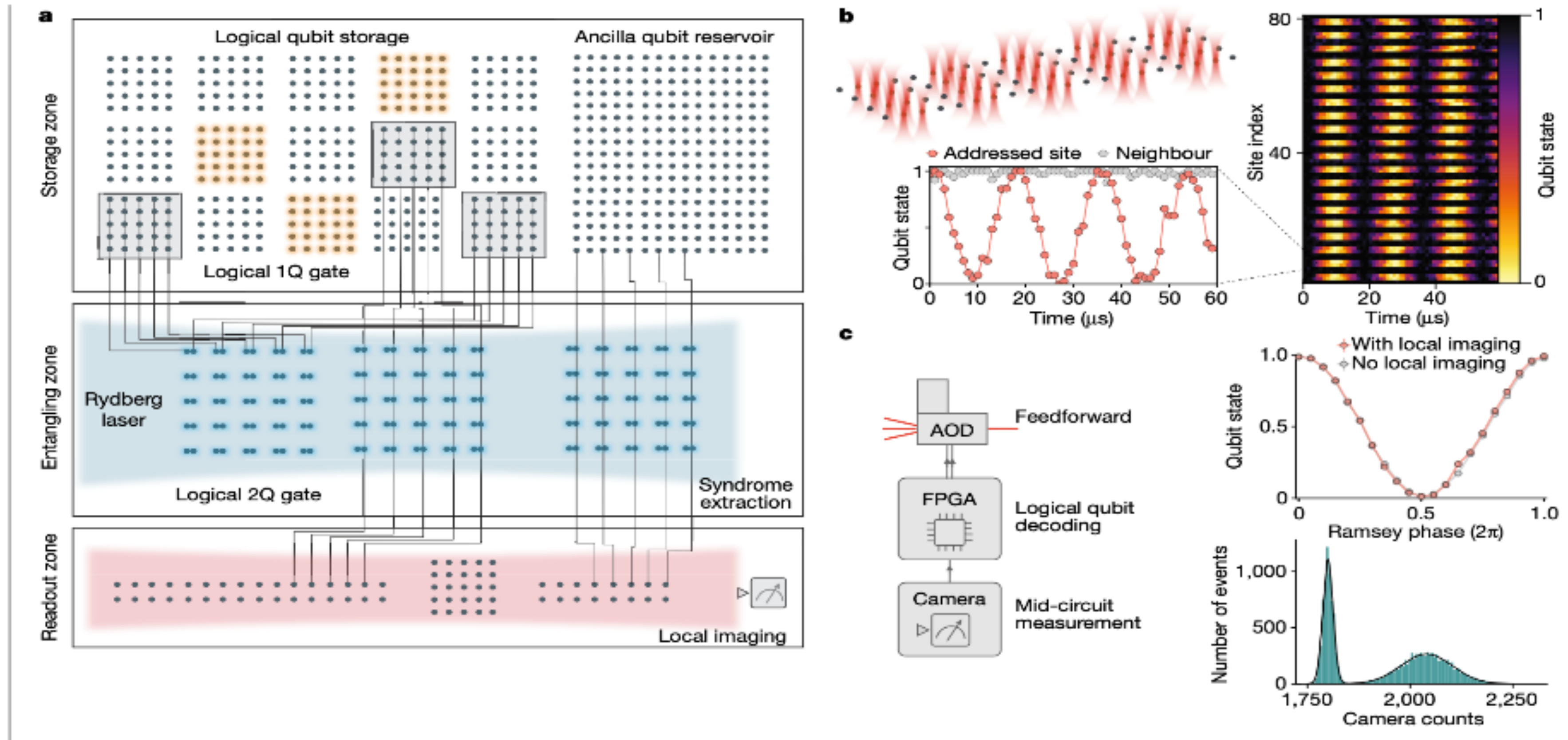


**Fig. 1 | A programmable logical processor based on reconfigurable atom arrays. a,** Schematic of the logical processor, split into three zones: storage, entangling and readout (see Extended Data Fig. 1 for detailed layout). Logical single-qubit and two-qubit operations are realized transversally with efficient, parallel operations. Transversal CNOTs are realized by interlacing two logical qubit grids and performing a single global entangling pulse that excites atoms to Rydberg states. Physical qubits are encoded in hyperfine ground states of $^{87}$Rb atoms trapped in optical tweezers. **b,** Fully programmable single-qubit rotations are implemented using Raman excitation through a 2D AOD; parallel grid illumination delivers the same instruction to multiple atomic qubits. **c,** Mid-circuit readout and feedforward. The imaging histogram shows high-fidelity state discrimination (500 μs imaging time, readout fidelity approximately 99.8%; Methods) and the Ramsey fringe shows that qubit coherence is unaffected by measuring other qubits in the readout zone (error probability $p \approx 10^{-3}$; Methods). The FPGA performs real-time image processing, state decoding and feedforward (Fig. 4).

# Nature 626 (2024) 58

# Quantum Computing in “noisy environment” or Fault–Tolerant QC

- Fighting quantum decoherence with entanglement
- Quantum Error Correction (QEC)

cf. B.M Terhal, Rev. Mod. Phys. 87 (2015) 307

# Fault-Tolerant Quantum Memory

Nature 627 (2024) 778

**Article**

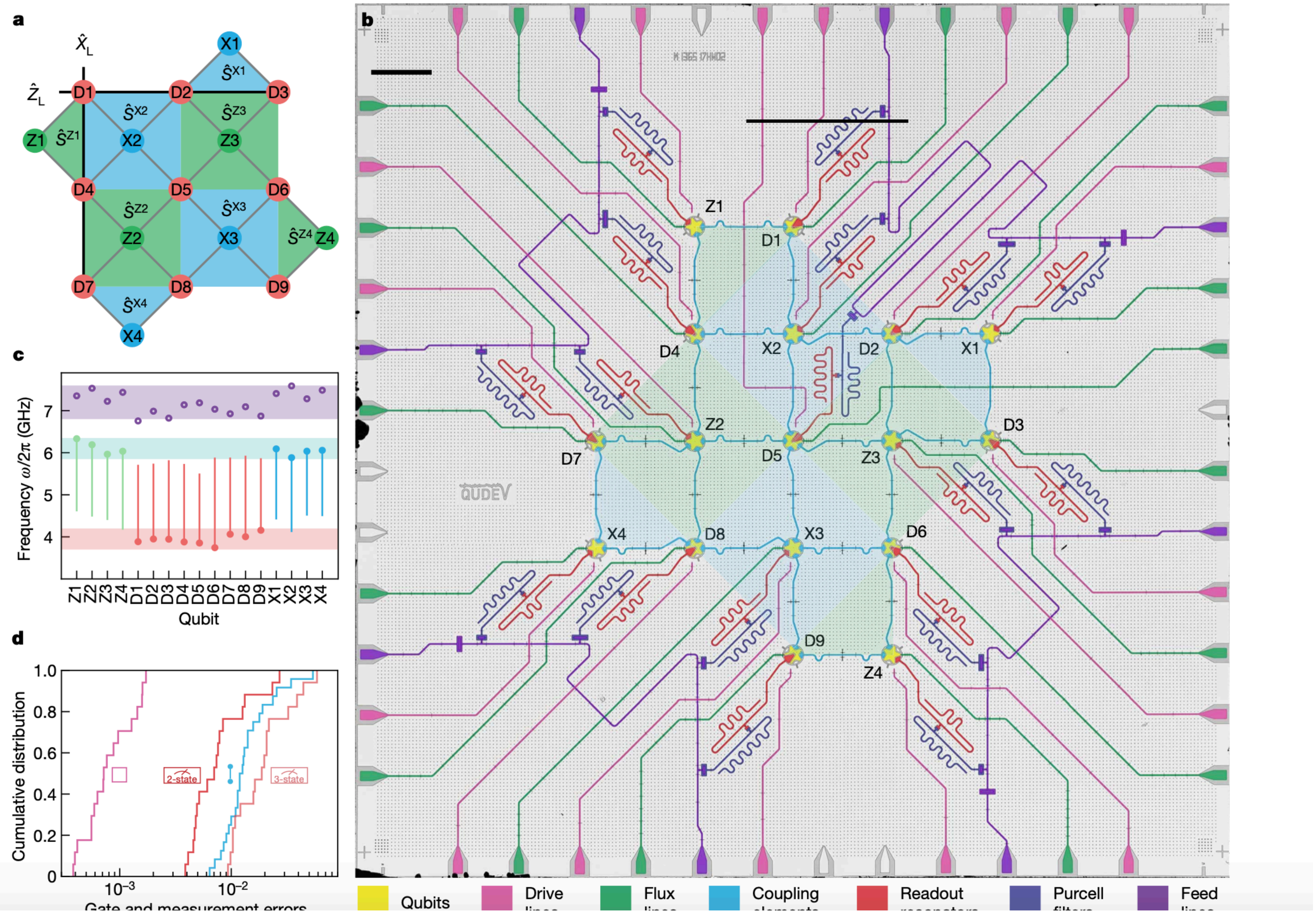


# Fault-Tolerant Universal Quantum Gate

Nature 605 (2022) 675

**Article**

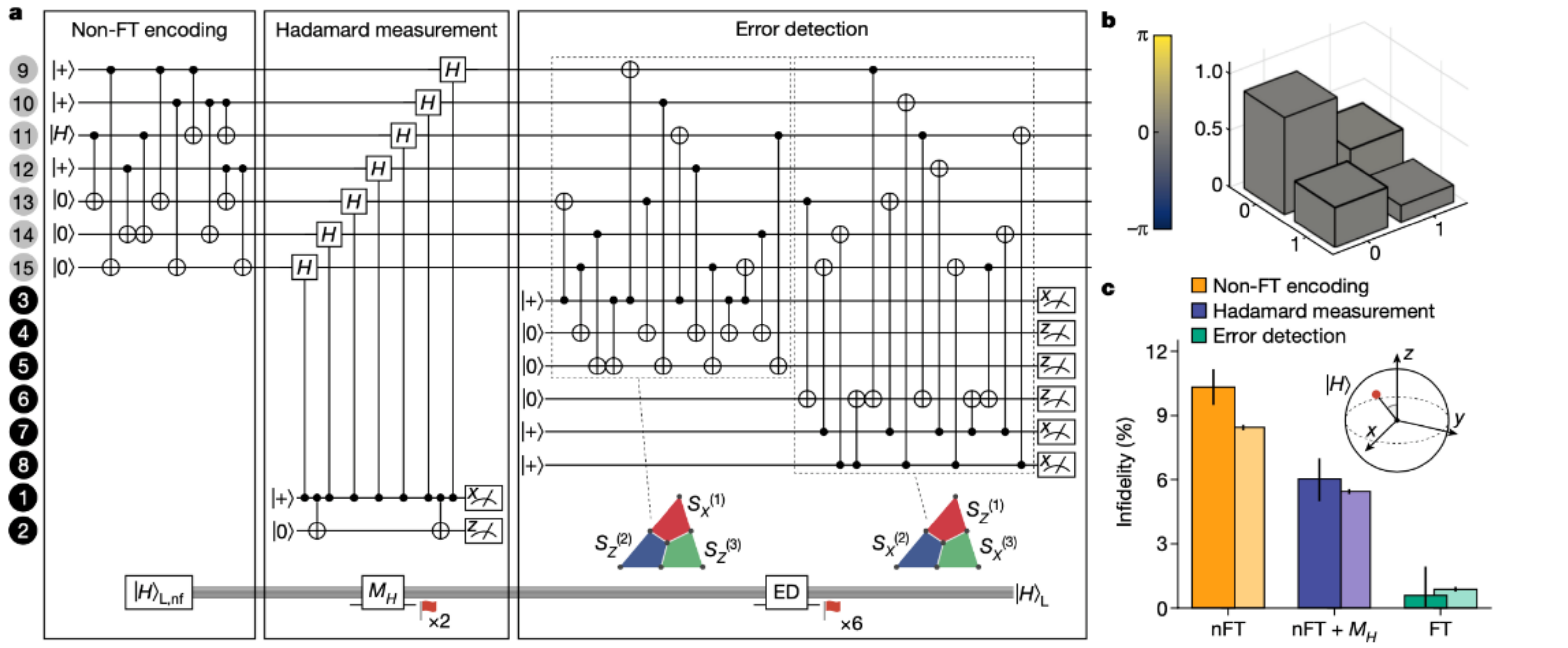


**Fig. 4 | Fault-tolerant generation of a logical magic state $|H\rangle_L$. a**, The magic state is prepared non-fault-tolerantly in a first step, where a physical magic state $|H\rangle$ is mapped to the logical state $|H\rangle_{L,nf}$ encoded in the data qubits at positions 9 to 15 in the ion string (see labels at left of circuit). Thereafter, a FT measurement of the Hadamard operator ($M_H$) is carried out. Two auxiliary qubits herald that the prepared state is a +1 eigenstate of the Hadamard operator but also that no dangerous error occurred during the measurement. The magic-state preparation is concluded with an error-detection (ED) block that measures the three *X*-type and *Z*-type stabilizers each in an FT fashion. The first part of the error-detection circuit (first dashed box), measures $S_X^{(1)}$, $S_Z^{(2)}$ and $S_Z^{(3)}$, whereas the second part measures $S_Z^{(1)}$, $S_X^{(2)}$ and $S_X^{(3)}$. The magic-state preparation is discarded and repeated in case of a non-trivial syndrome of the eight auxiliary qubits 1 to 8. **b**, Logical state tomography (see 'Transversal fault-tolerant operations') after FT magic-state preparation. The phase of the complex amplitudes is encoded in the colour of the three-dimensional bar plot and the wireframes depict ideal results. Phase deviations from the ideal density matrix are smaller than 50 mrad whereas amplitude deviations are smaller than 0.007. **c**, The decrease in infidelity of the logical magic state (red marker on Bloch sphere) after each step of the FT preparation procedure is observed experimentally and captured by depolarizing noise simulations (experimental and simulation results depicted darker and lighter, respectively).

# Quantum error and statistical model

- Specific quantum code with stabilizer formalism
- Modeling quantum error pattern
- Mapping quantum error pattern to statistical model
- cf. simple case: Dennis et al, J. Math. Phys. 43 (2002) 4452

# Quantum Error Detection/Correction

- Check whether error happens via the measurement of "ancilla" qubits: measurement result is called syndrome (quantum error detection)
- From the syndrome, guess quantum error probabilistically
- Correct quantum error

# Error rate and threshold probability

- If the quantum error rate is higher than the "threshold probability", QEC is not possible.
- Above the threshold probability, "probabilistic correction" is not possible.
- "Probabilistic interpretation" is related to some statistical model

# Warm-up: 1-D repetition code

- realistic quantum circuit diagram for 1-D repetition code with phase flip error and mapping to a statistical model (quenched 2-D Ising model on a triangular lattice)

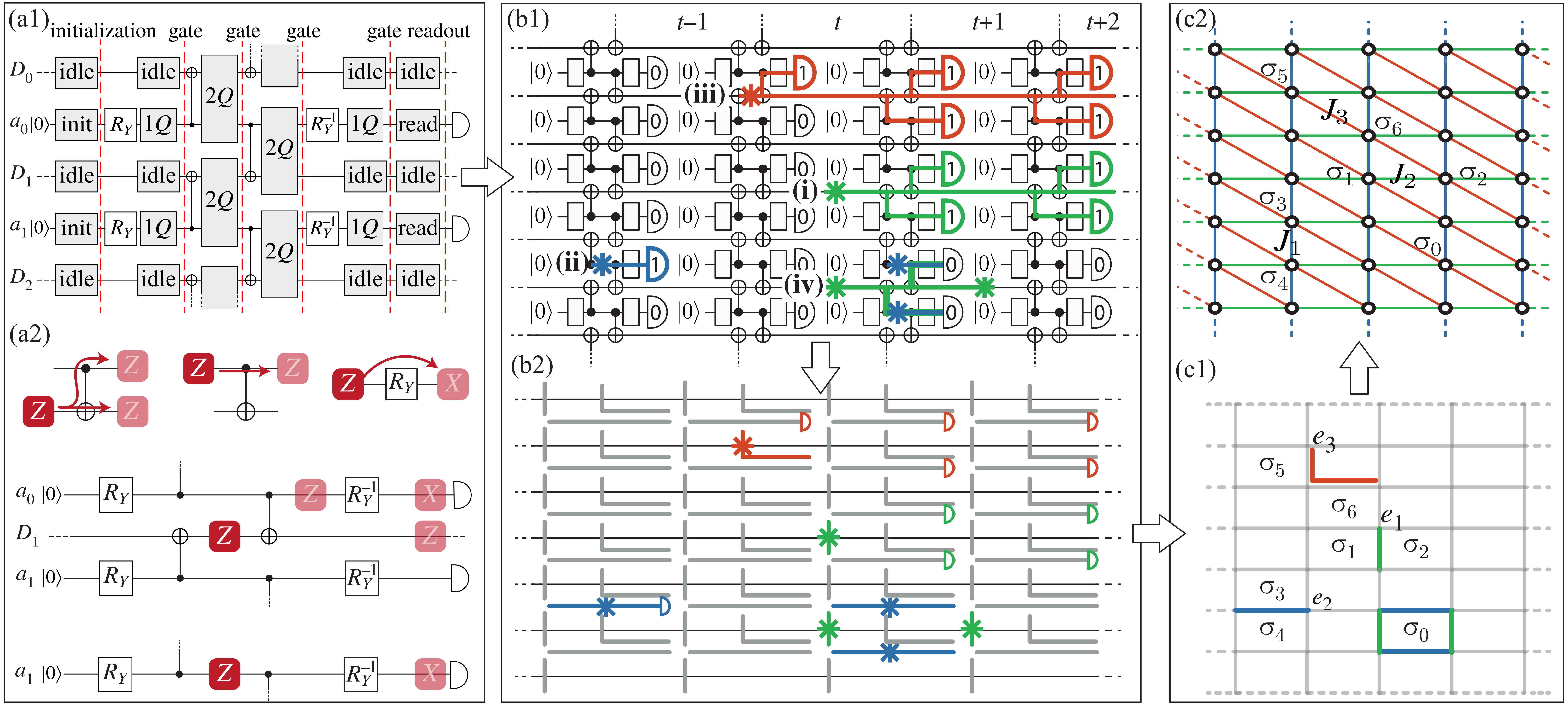

# Toric code circuit

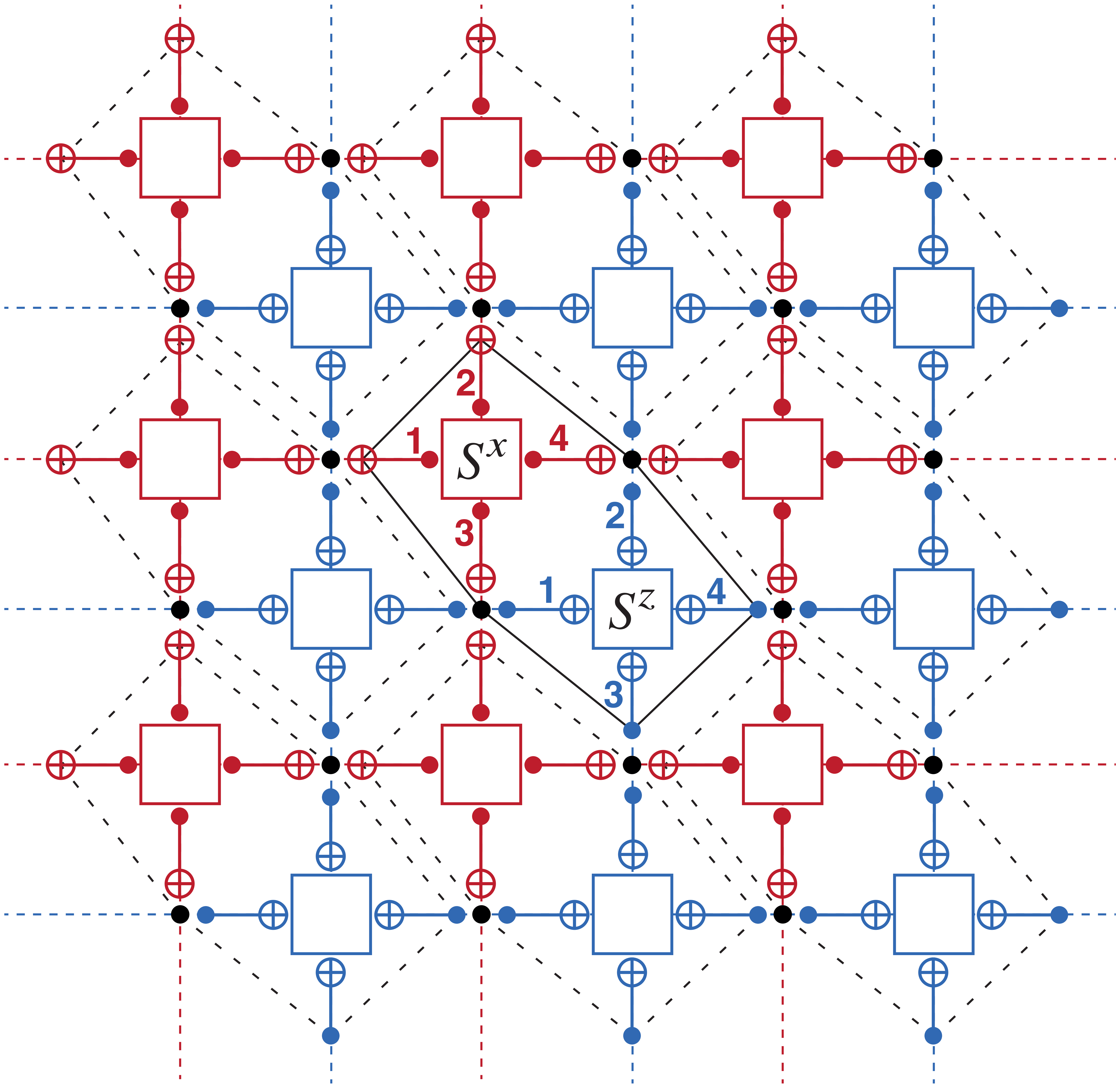

# Quantum Error Models and Mapped Statistical physics models in Toric Code

- Random bit flip ($\sigma_x$) error or phase flip ($\sigma_z$) error

  —〉 2–D Ising model with quenched anti–ferromagnetic coupling

- Random bit flip error or phase flip error + syndrome measurement error

  —〉 3–D $Z(2)$ gauge theory with quenched anti–ferromagnetic coupling

# Quantum Error Models and Mapped Statistical physics models in Toric Code

- Independent $(\sigma_x)$, $(\sigma_z)$ error + syndrome measurement error

  —〉 3−D $Z(2)$ gauge theory

  with quenched anisotropic anti−ferromagnetic coupling

- Depolarizing (i.e., $(\sigma_x)$,$(\sigma_y)$,$(\sigma_z)$) error + syndrome measurement error

  —〉 3−D $Z(2) \times Z(2)$ gauge theory

  with anisotropic quenched anti−ferromagnetic coupling

# Polyakov Line, $Z(2) \times Z(2)$ gauge theory

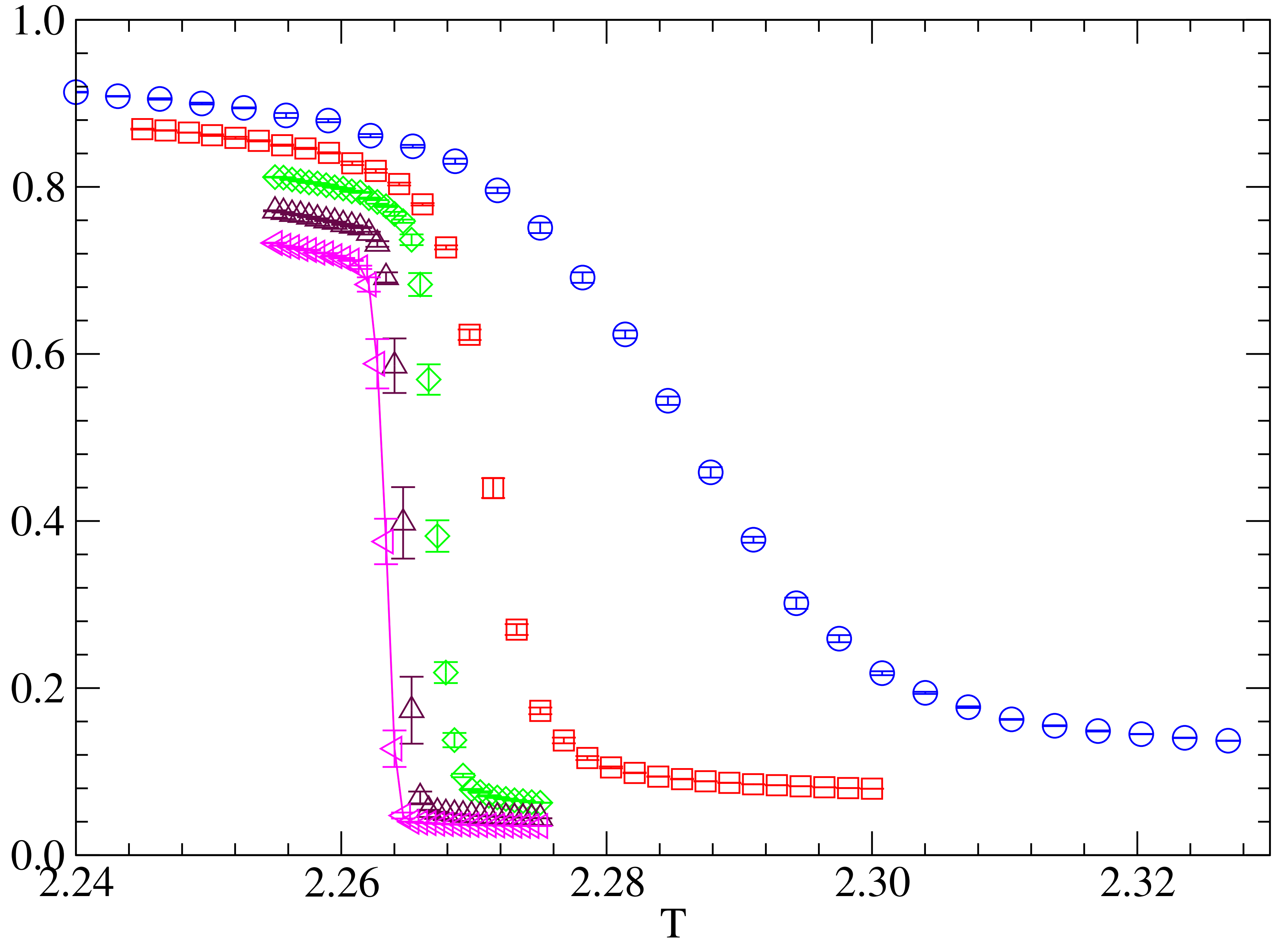


P = 2.88 x 10-5

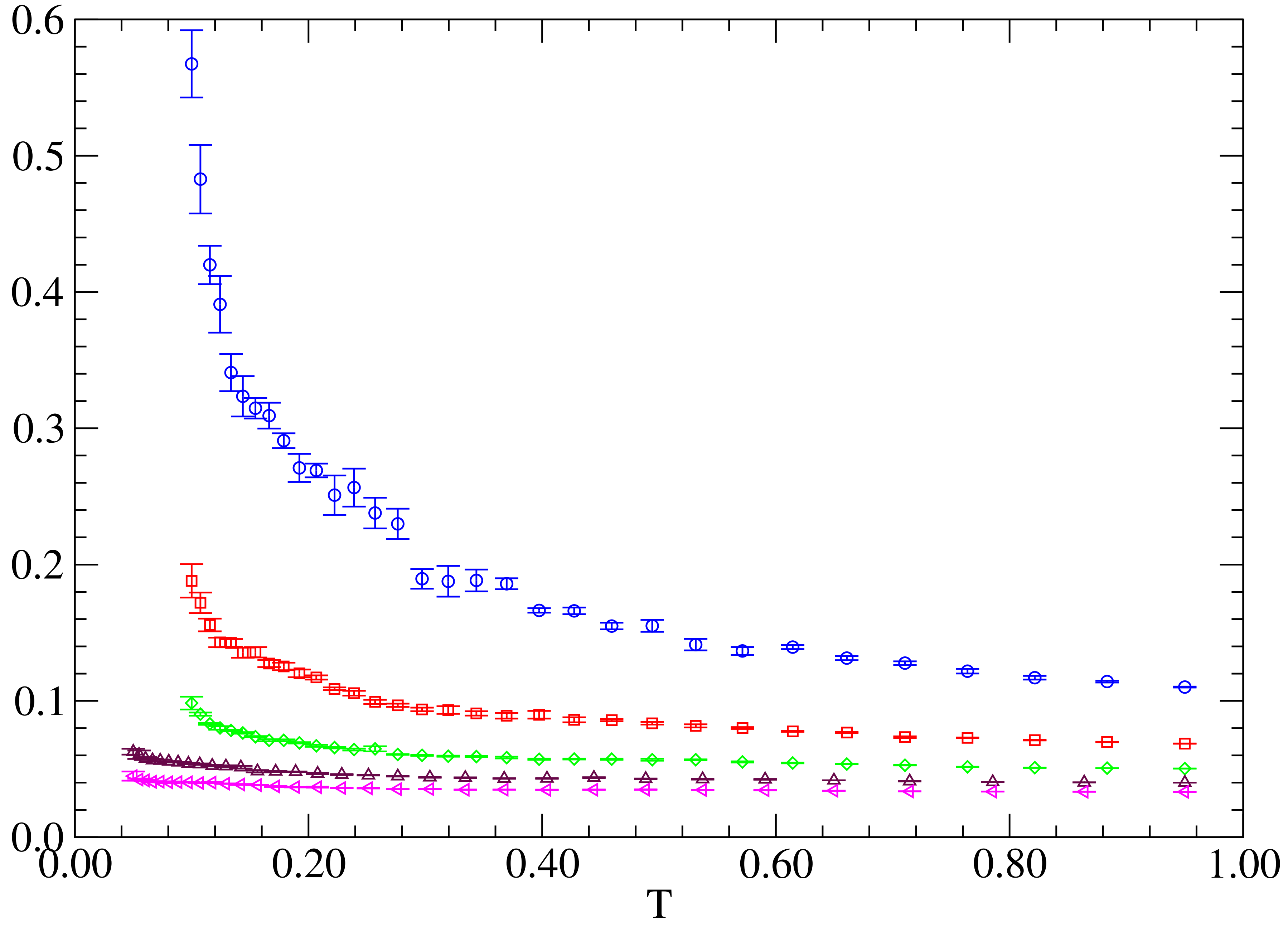


P = 0.0231

# Third order cumulant of Polyakov Line, $Z(2) \times Z(2)$ gauge theory

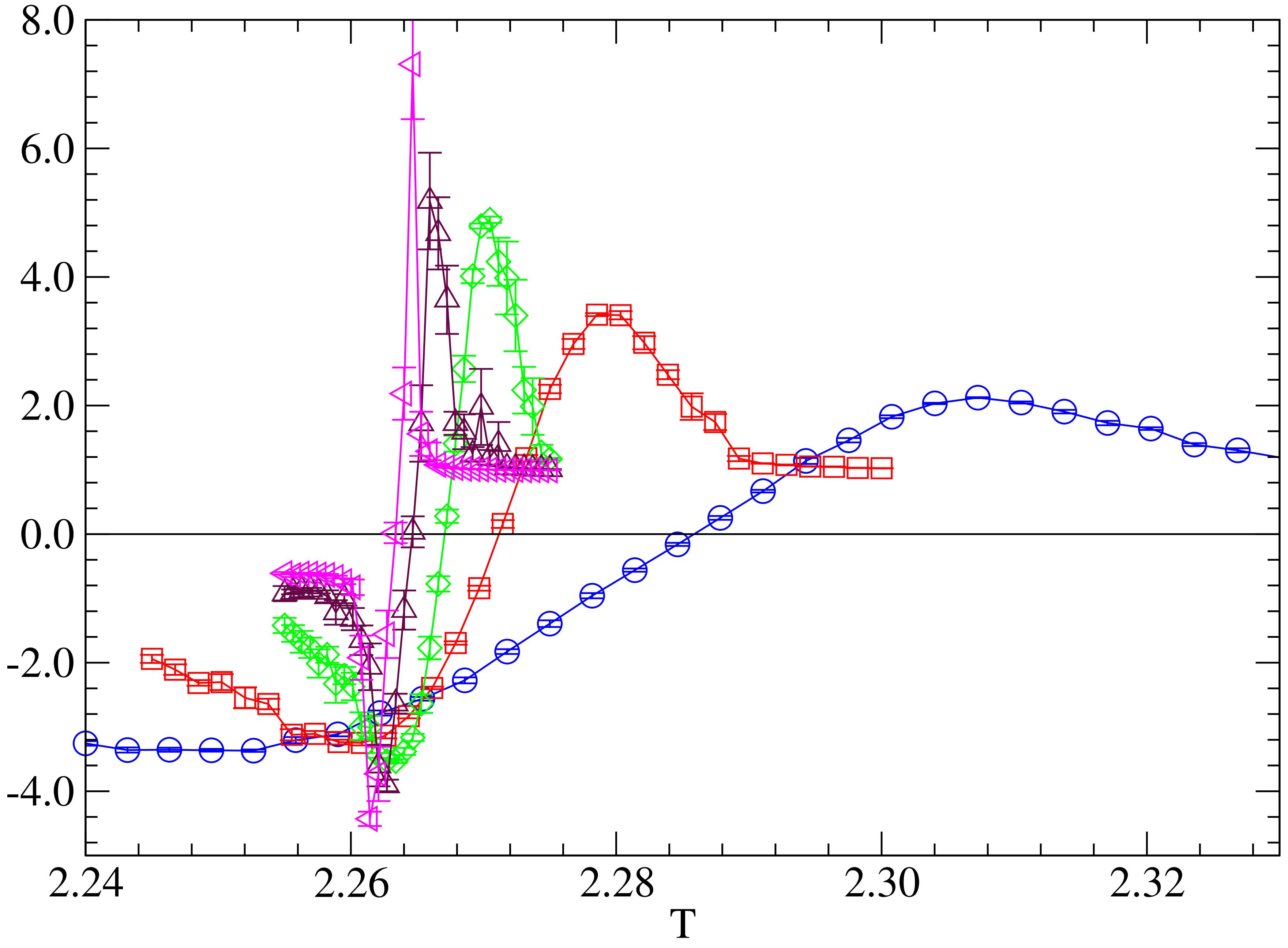


P = 2.88 x 10-5

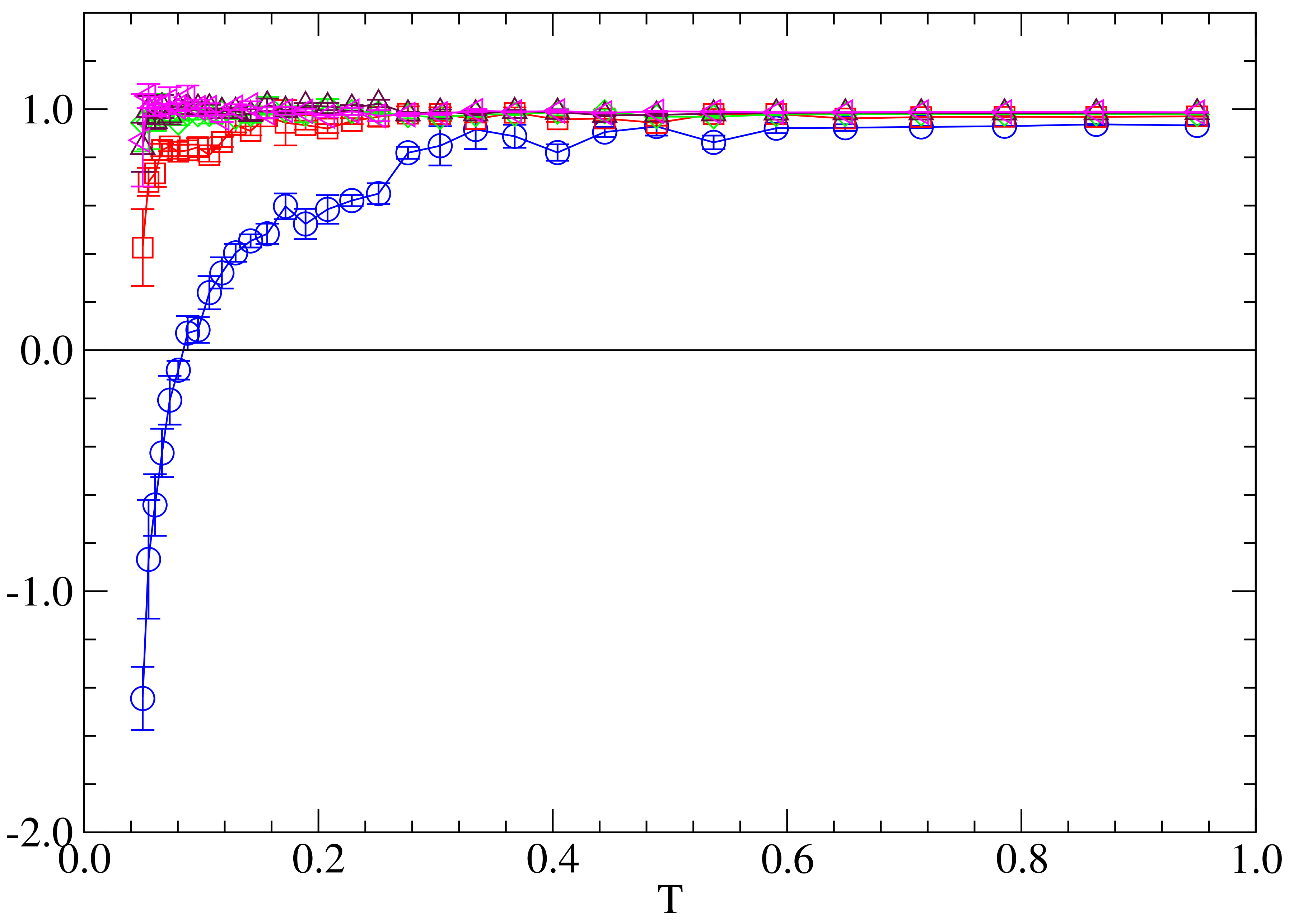


P = 0.0231

# Susceptibility of Polyakov Line, $Z(2) \times Z(2)$ gauge theory

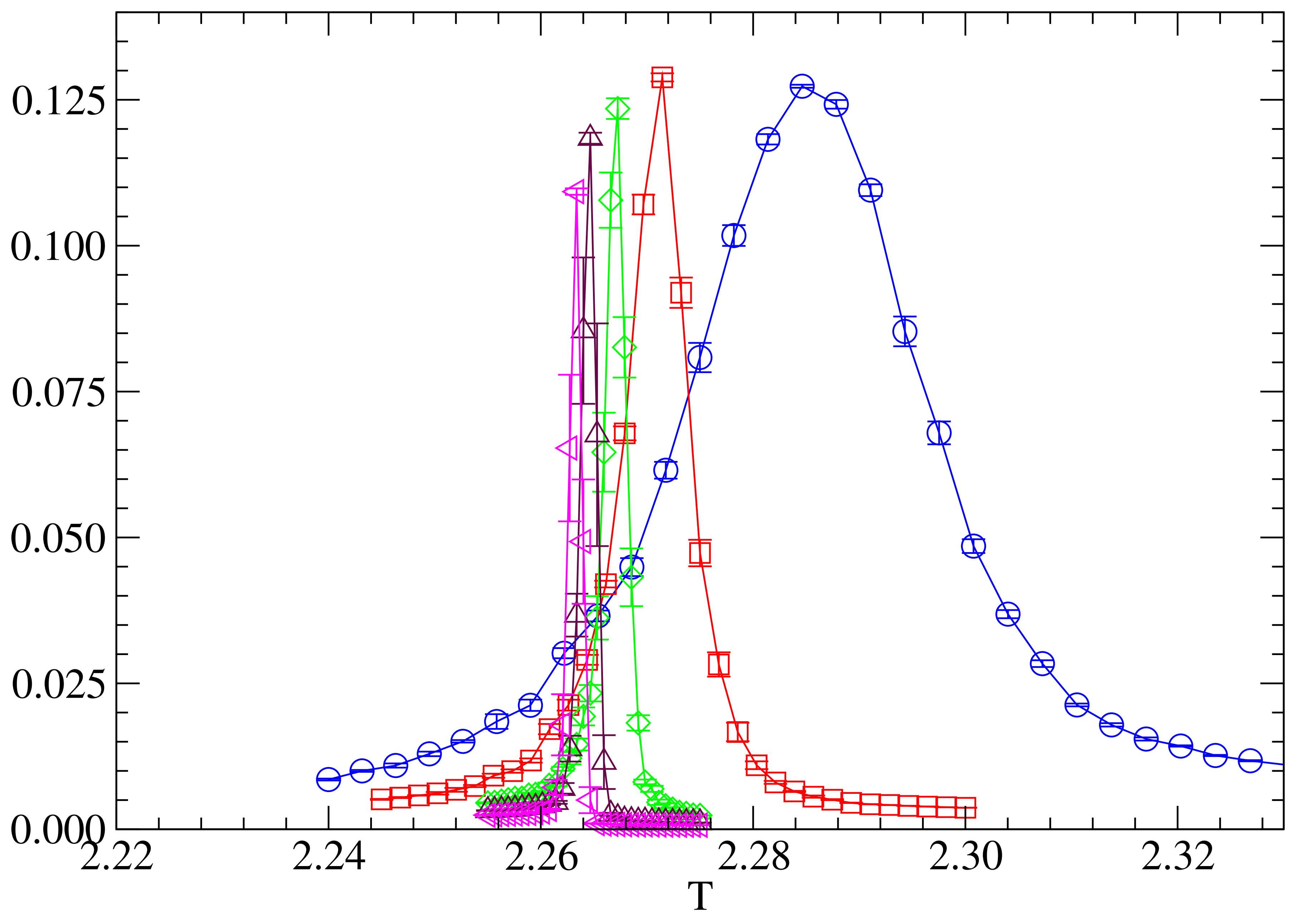


P = 2.88 x 10-5

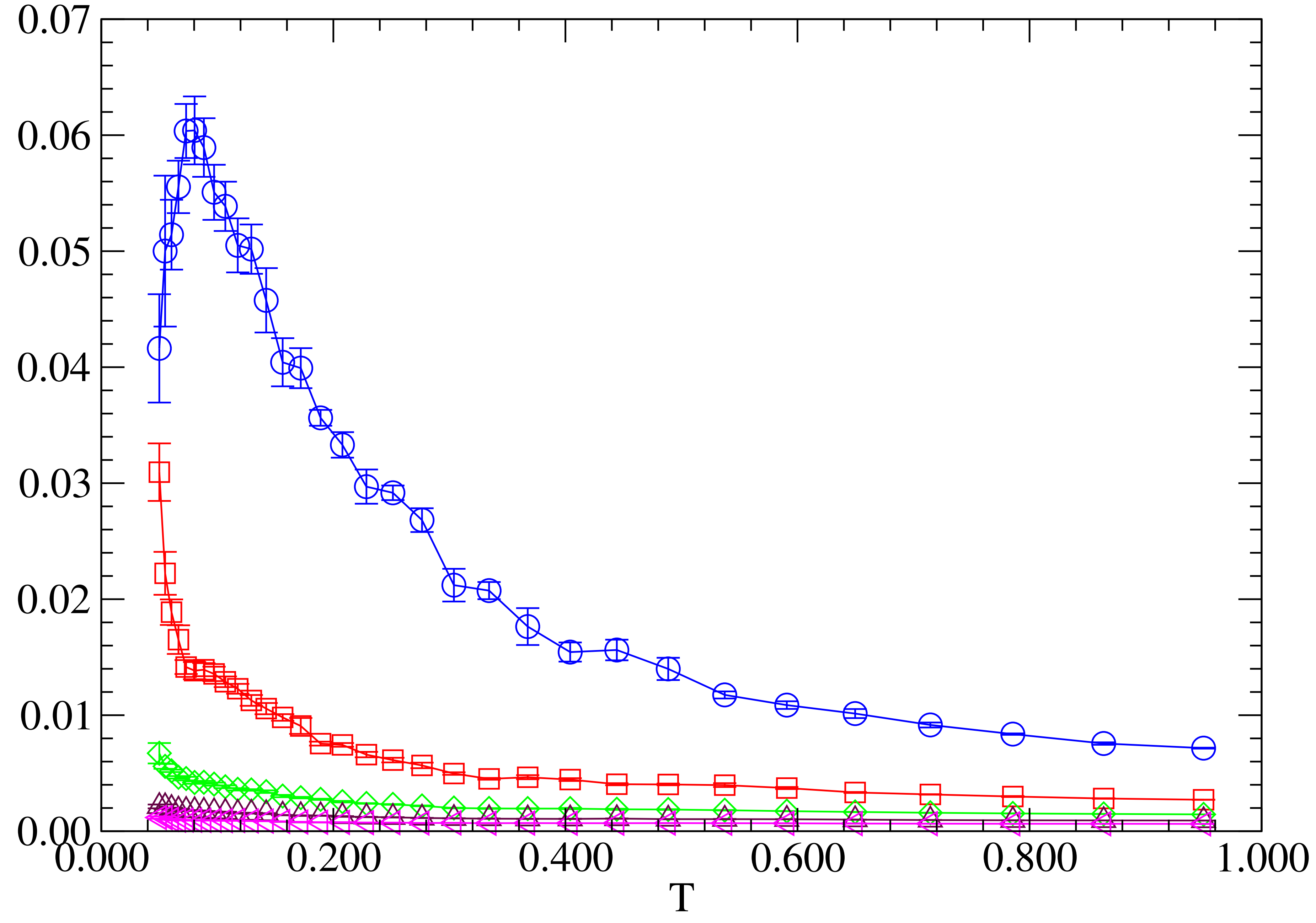


P = 0.0231

# Phase diagram, $Z(2) \times Z(2)$ gauge theory

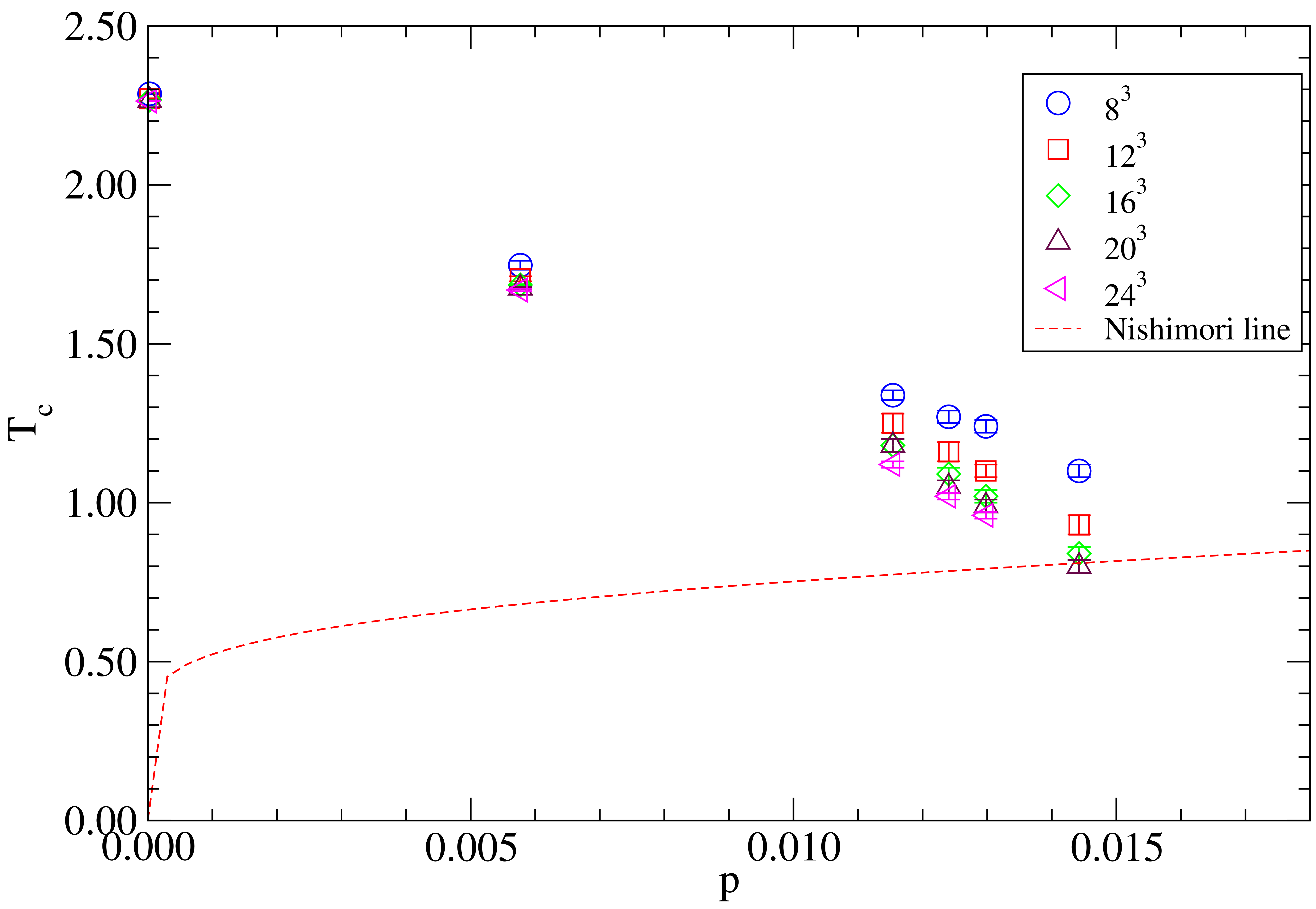

# Conclusion

- Threshold error probability for the viability of Quantum Error Correction can be studied by MC simulation of quenched statistical physics model
- For toric code where an independent bit−flip or phase flip occurs together with independent syndrome measurement error, the threshold probability from MC suggests $p \sim 0.00682$
- For toric code where depolarizing noise occurs together with independent syndrome measurement error, the threshold probability from MC suggests $p \sim 0.0144$